Three BUB1 and BUBR1/MAD3-related spindle assembly checkpoint proteins are required for accurate mitosis in Arabidopsis

ARTICLE *in* NEW PHYTOLOGIST · SEPTEMBER 2015

Impact Factor: 6.55 · DOI: 10.1111/nph.13073

10 AUTHORS, INCLUDING:

Marie-cecile Caillaud
Ecole normale supérieure de Lyon
14 PUBLICATIONS **615** CITATIONS
SEE PROFILE

Isabelle Damiani
French National Institute for Agricultural R…
10 PUBLICATIONS **252** CITATIONS
SEE PROFILE

Pavel A Karpov
National Academy of Sciences of Ukraine
26 PUBLICATIONS **33** CITATIONS
SEE PROFILE

Bruno Favery
French National Institute for Agricultural R…
36 PUBLICATIONS **1,520** CITATIONS
SEE PROFILE

New Phytologist

Research

Three BUB1 and BUBR1/MAD3-related spindle assembly checkpoint proteins are required for accurate mitosis in Arabidopsis

Laetitia Paganelli[1,2,3], Marie-Cécile Caillaud[4], Michaël Quentin[1,2,3], Isabelle Damiani[1,2,3], Benjamin Govetto[1,2,3], Philippe Lecomte[5], Pavel A. Karpov[6], Pierre Abad[1,2,3], Marie-Edith Chabouté[7] and Bruno Favery[1,2,3]

[1]UMR 1355, Institut Sophia Agrobiotech, INRA, 400 route des Chappes, F-06903 Sophia-Antipolis, France; [2]UMR 7254, CNRS, 400 route des Chappes, F-06903 Sophia-Antipolis, France; [3]UMR 1355, Université de Nice Sophia-Antipolis, 400 route des Chappes, F-06903 Sophia-Antipolis, France; [4]The Sainsbury Laboratory, John Innes Centre, Norwich Research Park, Norwich NR4 7UH, UK; [5]UMR 1095, INRA – Université Blaise Pascal, Génétique, Diversité et Ecophysiologie des Céréales, F-63039, Clermont Ferrand, France; [6]Institute of Food Biotechnology and Genomics, National Academy of Sciences of Ukraine, Kiev, Ukraine; [7]CNRS, Institut de Biologie Moléculaire des Plantes, Unité Propre de Recherche 2357 Conventionné avec l'Université de Strasbourg, F-67084 Strasbourg, France

Author for correspondence:
Bruno Favery
Tel: +33 492 386464
Email: favery@sophia.inra.fr

Received: *5 February 2014*
Accepted: *27 July 2014*

New Phytologist (2014)
doi: 10.1111/nph.13073

Key words: cell cycle, checkpoint, giant cell, kinetochore, mitosis, nematode.

Summary

- The spindle assembly checkpoint (SAC) is a refined surveillance mechanism which ensures that chromosomes undergoing mitosis do not segregate until they are properly attached to the spindle microtubules (MT). The SAC has been extensively studied in metazoans and yeast, but little is known about its role in plants.
- We identified proteins interacting with a MT-associated protein MAP65-3, which plays a critical role in organising mitotic MT arrays, and carried out a functional analysis of previously and newly identified SAC components.
- We show that Arabidopsis SAC proteins BUB3.1, MAD2, BUBR1/MAD3s and BRK1 interact with each other and with MAP65-3. We found that two BUBR1/MAD3s interacted specifically at centromeres. When stably expressed in Arabidopsis, BRK1 localised to the kinetochores during all stages of the mitotic cell cycle. Early in mitosis, BUB3.1 and BUBR1/MAD3.1 localise to the mitotic spindle, where MAP65-3 organises spindle MTs. A double-knockout *mad3.1 mad3.2* mutant presented spindle MT abnormalities, chromosome misalignments on the metaphase plate and the production of lagging chromosomes and micronuclei during mitosis.
- We conclude that BRK1 and BUBR1/MAD3-related proteins play a key role in ensuring faithful chromosome segregation during mitosis and that their interaction with MAP65-3 may be important for the regulation of MT-chromosome attachment.

Introduction

Cell division is a highly regulated process that requires surveillance mechanisms, to ensure that both daughter cells receive one copy of each chromosome before the initiation of anaphase, in particular. The spindle assembly checkpoint (SAC) is a conserved monitoring system for the eukaryotic cell cycle that prevents chromosome missegregation by delaying the metaphase-to-anaphase transition until all chromosomes are properly bi-oriented on the mitotic spindle (Musacchio & Salmon, 2007; Khodjakov & Rieder, 2009). Key components of the SAC include BUDDING UNINHIBITED BY BENZYMIDAZOL 1 and 3 (BUB1 and BUB3), BUB1-related (BUBR1) or MITOSIS ARREST DEFECT 3 (MAD3), and MAD2 (Musacchio & Salmon, 2007). The kinetochore is at the heart of the SAC. This specialised protein complex assembles on centromeric DNA and provides a site for chromosome binding to spindle microtubules (MT) early in mitosis. In higher organisms, SAC proteins localise to unattached kinetochores at this stage (Cleveland *et al.*, 2003; Howell *et al.*, 2004). As long as there are unattached kinetochores unable to produce sufficient tension between sister chromatids, the SAC conditions remain unsatisfied and the mitotic checkpoint complex (MCC) is generated. The MCC is the main effector of the SAC, acting by the sequestration and inhibition of CDC20 (CELL-DIVISION CYCLE PROTEIN 20), which is responsible for triggering the metaphase-to-anaphase transition (Sudakin *et al.*, 2001; Pines, 2011). Once the checkpoint conditions are satisfied by MT-attachment and tension, APC/C inhibition by MCC, via CDC20, is rapidly released, in a process known as checkpoint silencing (Musacchio, 2011).

Plant SAC protein homologues were initially identified *in silico* (Houben & Schubert, 2003; Caillaud *et al.*, 2009). Plant

MAD2 homologues have been shown to localise to chromosome kinetochores during early mitosis, suggesting that this pathway is conserved in higher plants (Yu *et al.*, 1999; Kimbara *et al.*, 2004). In *Arabidopsis thaliana, BUB3.1*, *BUBR1*/*MAD3.1* and *MAD2* transcript levels display a distinct peak at the G2/M boundary in synchronised cell cultures (Menges *et al.*, 2005) and the expression of these genes *in planta* is restricted to meristematic tissues (Caillaud *et al.*, 2009). As in metazoans and yeast, the BUB3.1, BUBR1/MAD3.1 and MAD2 proteins of Arabidopsis interact physically with each other (Caillaud *et al.*, 2009). As expected, they localise to unattached kinetochores when the conditions of the SAC remain unsatisfied due to global defects in spindle assembly as demonstrated for example, in *Xenopus* (Chen *et al.*, 1996) and in humans (Taylor *et al.*, 1998). In cases of 'delayed anaphase', BUB3.1, BUBR1/MAD3.1 and MAD2 associate with both kinetochores and kinetochore MTs *in vivo*, suggesting a possible interaction between SAC proteins and the MT-associated proteins (MAPs) organising the mitotic spindle (Caillaud *et al.*, 2009). The recent characterization of a completely sterile mutant of *Oryza sativa* (rice) made it possible to identify a kinetochore-localised BUB1 homologue, BRK1 (BUB1-related protein kinase 1), as essential for generation of the correct tension between homologous kinetochores at metaphase I of meiosis (Wang *et al.*, 2012). In Arabidopsis, *bub3.1* knockout (KO) plants have an embryo-lethal phenotype, highlighting the key role of this gene in gametophyte development or embryogenesis (Lermontova *et al.*, 2008). However, little is known about the role of SAC in plant mitosis.

An interesting model system for studies of the role of genes involved in cell cycle regulation and cytoskeleton dynamics (De Almeida Engler *et al.*, 2011; De Almeida-Engler & Favery, 2011; Masoud *et al.*, 2013) is the ontogenesis of hypertrophied multinucleate feeding giant cells induced by root-knot nematodes (Caillaud *et al.*, 2008). Multiple spindles are observed in giant cells and time-lapse studies *in vivo* have revealed the presence in mitotic giant cells of early synchronous phragmoplast MT arrays that do not develop any further (Caillaud *et al.*, 2008). Detailed functional analyses of genes differentially expressed in giant cells have shown that the Arabidopsis MT-associated protein MAP65-3 plays a critical role in plant cell division and giant cell development (Müller *et al.*, 2004; Caillaud *et al.*, 2008). Unlike animal and fungal genomes, which contain one or two MAP65/Ase1p/PRC1 homologues, the Arabidopsis genome contains a family of nine MAP65 genes (Hussey *et al.*, 2002; Smertenko *et al.*, 2008). In the absence of functional MAP65-3, giant cells begin to develop but do not complete their differentiation and are eventually destroyed (Caillaud *et al.*, 2008). MAP65-3 plays a key role in MT array organisation during both mitosis (spindle morphogenesis) and cytokinesis (phragmoplast expansion) in all dividing plant cells. MAP65-1, -2 and -3 have been shown to be a substrate of the mitogen-activated protein kinase MPK4 in Arabidopsis (Kosetsu *et al.*, 2010; Sasabe *et al.*, 2011). MAP65-3 acts as an MT-bundling factor that specifically cross-links antiparallel MTs near their plus ends during the establishment of the phragmoplast MT array (Ho *et al.*, 2012).

In this study, we used a yeast two-hybrid (Y2H) screen to identify proteins interacting with MAP65-3. We demonstrated physical interactions between MAP65-3 and central components of the SAC and studied their co-expression during plant development and in response to root-knot nematode infection. To investigate the functions of BUBR1/MAD3.1 and the two novel components of the Arabidopsis SAC, MAD3.2 and BRK1, we studied their subcellular localisation *in planta* and analysed mitosis in *mad3.1, mad3.2* and *brk1* single and multiple mutants. Our results demonstrated the conservation of BUBR1/MAD3.1, MAD3.2 and BRK1 functions in the regulation of the SAC mechanism underlying basal mitotic timing and promoting correct kinetochore-MT linkage to ensure the fidelity of chromosome segregation during mitosis in plants.

Materials and Methods

Plant materials, growth conditions and nematode infection

Arabidopsis WT ecotypes and T-DNA insertion lines were obtained from the Nottingham Arabidopsis Stock Centre (GABI_084G06 in Columbia Col0 background ecotype) and the INRA Institute in Versailles, France (DQH17 and EII34 in the Wassilewskija WS background ecotype). The ProMAD3.1, ProMAD2 and ProBUB3.1:GFP:GUS lines were generated as part of a previous study (Caillaud *et al.*, 2009). For *in vitro* analyses, seeds were surface-sterilised and grown on MS medium containing 1% sucrose, 0.7% plant cell culture-tested agar (Sigma), and 50 μg ml^{-1} kanamycin. Kanamycin resistance was scored in 2-wk-old seedlings. For nematode infection *in vitro*, 100 surface-sterilised freshly hatched *Meloidogyne incognita* second-stage juveniles (J2) were added to each 2-wk-old seedling. The plates were kept at 20°C, with a 16-h photoperiod. All of the observations reported were obtained in three independent experiments. Tobacco (*Nicotiana benthamiana*) plants were grown under continuous light for 1 month at 26°C. Tobacco leaves were infiltrated with *Agrobacterium tumefaciens*, as previously described (Caillaud *et al.*, 2009), and plants were analysed 2 d after infiltration. For drug treatment, we used oryzalin (Sigma) at a final concentration of 150 nM. Homozygous plants were crossed with Pro_{35S}*:MBD:GFP,* Pro_{35S}*:HTR12:GFP* or Pro_{35S}*:H2B:YFP Arabidopsis* plants. Plants expressing the two constructs were obtained and used for microscopy analysis.

Gene and promoter cloning and RT-qPCR analysis

Arabidopsis thaliana proteins orthologous to human BUB1 were identified by BLASTP analysis. Interpro scans (http://www.ebi.ac.uk/interpro) were used to study domain organisation. The *A. thaliana MAD3.2* and *BRK1* coding sequences were amplified by PCR, with specific primers (Supporting Information Table S1). They were inserted into the pDON207 donor vector and then into the pK7FWG2, PK7GWF2 plant expression and BiFC vectors (pAM-35SS-GWY-YFPc and pAM-35SS-GWY-YFPn), with Gateway Technology (Invitrogen). For the promoter-GUS fusion, 1-kb fragments immediately upstream from the start

codon were amplified by PCR, inserted into the pDON207 donor vector and then into the pKGWFS7 plant vector. For the expression of GFP fusions under the control of the MAP65-3 promoter, the Pro_{35S} *Hin*dIII/*Spe*I fragment of the pK7WGF2 and pK7FWG2 vectors (Karimi *et al.*, 2002) was replaced with $Pro_{MAP65\text{-}3}$, as previously described (Caillaud *et al.*, 2008). For RT-qPCR, total RNA was extracted from nonmeristematic root and gall tissues from *A. thaliana* cv WS dissected at various time points after nematode inoculation (7, 14, 21 d post infection, dpi). RT-qPCR analyses were performed as previously described (Jammes *et al.*, 2005), in the Opticon 2 system (MJ research; Bio-Rad). At5g10790 (*UBP22*) and At5g62050 (*OXA1*) were used to normalise RT-qPCR data (Table S1). Three independent quantitative RT-PCRs were carried out per sample and three biological replicates were performed.

Histochemical localisation of GUS activity and microscopic analyses

Wild-type (WS ecotype) *A. thaliana* plants were stably transformed and GUS activity was assayed histochemically, as previously described (Caillaud *et al.*, 2008), on at least five independent transformed plants for each construct. Galls, root apices and shoot apical meristems were dissected from GUS-stained plants, fixed in 1% glutaraldehyde and 4% formaldehyde in 50 mM sodium phosphate buffer, pH 7.2, dehydrated, and embedded in Technovit 7100 (Heraeus Kulzer, Wehrheim, Germany), as described by the manufacturer. Sections (4 μm thick) were stained with 0.05% ruthenium red and mounted in DPX (BDH Laboratory Supplies, VWR International, Fontenay-sous-Bois, France). Samples were observed with a Zeiss Axioplan 2 microscope (Jena, Germany) and images were analysed with AxioVision 4.7 (Zeiss). Optical sections of tobacco leaf epidermal cells or tobacco cell cultures were observed with a ×63 water immersion apochromatic objective (numerical aperture 1.2; Zeiss) fitted to an inverted confocal microscope (model LSM510; Zeiss) at 25°C. The FM4-64 fluorescent dye (Molecular Probes, Grand Island, NY, USA) was used at a final concentration of 1 μM. The fluorescence of GFP, YFP and FM4-64 was monitored in channel mode with a BP 505-530, 488 beam splitters and LP 530 filters for GFP. For mutants, plantlets were fixed according to the protocole described by Janski *et al.* (2012) and stained using 0.1 mg ml^{-1} 4,6′-diamidino-2-phenylindole (DAPI). The fluorescence of H2B-YFP and MBD-GFP was visualized on living seedlings mounted in propidium iodide (IP). Seedlings were observed with a Zeiss LSM 780 confocal microscope in multitracking mode which is able to specifically discriminate each fluorochrome signature (Carl ZeissAG, Le Pecq, France). GFP, YFP fusion proteins and IP fluorescences were collected with laser excitations of 488, 514, 561 nm and emission ranges of 493–516, 517–561 and 564–697 nm, respectively. The immunolocalisations were performed using rabbit polyclonal CENH3/HTR12 antibodies (1 : 500) (Talbert *et al.*, 2002) and secondary Alexa Fluor® 594 goat anti-rabbit IgG (Molecular Probes) as previously described (Caillaud *et al.*, 2009). For drug treatment, digital images were acquired with an AxioCam HRc camera (Zeiss) and analysed with LSM Image Browser (Zeiss).

Yeast two-hybrid split-ubiquitin assay

The split-ubiquitin assay was carried out in *Saccharomyces cerevisiae* strain JD53, as previously described (Caillaud *et al.*, 2009). The *BUB3.1, MAD2, BUBR1/MAD3.1, MAD3.2* and *BRK1* coding sequences were inserted into the GW:Cub:URA3 bait vector (pMKZ) and the NuI:GW prey vector, using the Gateway system. Standard procedures were used for yeast growth and transformation. Transformants were selected on 5-fluoroorotic acid (5-FOA) plates containing minimal medium with yeast nitrogen base without amino acids (Difco) and glucose, supplemented with lysine, leucine, uracil (M-HT) and 1 mg ml^{-1} 5-fluoroorotic acid (5-FOA).

3-D models

Kinase domain 3-D models were built in Modeller 9.12 using template Protein Data Bank structures: 3E7E, 3HMN and 4IJP. Molecular dynamics (MD) simulations and structure verification protocols were identical to those described earlier (Karpov *et al.*, 2010). MD computations were performed on IFBG Cluster (http://grid.ifbg.org.ua) of the VO CSLabGrid (http://infrastructure.kiev.ua/en/monitoring/47/). Molecular visualization and structural analysis was performed in PyMol 1.5 (www.pymol.org).

Accession numbers

Arabidopsis MAP65-3 (AT5G51600), MAD2 (AT3G25980), BUB3.1 (AT3G19590), BUBR1/MAD3.1 (AT2G33560), MAD3.2 (AT5G05510), BRK1 (AT1G20635; Uniprot F4IVI0), HTR12/CENH3 (AT1G01370), rice BRK1 (OS07G32480, EEC82122) and grape BRK1 (CBI21878).

Results

MAP65-3 interacts with conserved SAC complex subunits in Arabidopsis

Arabidopsis MAP65-3 (AT5G51600) was used as bait, to screen split-ubiquitin Y2H Arabidopsis cDNA libraries generated from mRNAs isolated from dissected galls or inflorescences obtained 7 d post *M. incognita* infection (7 dpi). We identified an interaction between the SAC subunit BUB3.1 and MAP65-3. We checked the specificity of this interaction, by investigating interactions between BUB3.1 and other members of the MAP65 family by Y2H screening (Fig. 1). We detected no interactions between BUB3.1 and MAP65-1, MAP65-4, MAP65-5 or MAP65-8, confirming the specificity of the interaction between BUB3.1 and MAP65-3.

We then investigated the possible interaction of MAP65.3 with other SAC subunits. We studied the previously identified

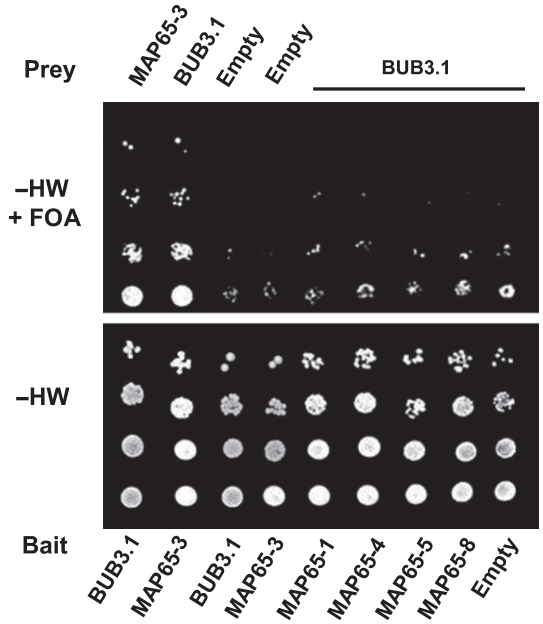

Fig. 1 Specific interaction between MAP65-3 and BUB3.1 in the yeast two-hybrid (Y2H) split-ubiquitin system. Dilution series of yeast JD53 cells expressing both bait:Cub:URA3 fusions and Nub:prey fusions were grown on yeast medium minus histidine and tryptophan (-HW) but containing 5-fluoroorotic acid (5-FOA), as indicated. The specific interaction between MAP65-3 and BUB3.1 resulted in uracil auxotrophy and 5-FOA resistance. No interactions were detected with MAP65-1, -4, -5 or -8.

MAD2 and BUBR1/MAD3.1 proteins (Caillaud *et al.*, 2009) and two additional new BUB1/BUBR1/MAD3-related proteins by Y2H screening. The Arabidopsis MAD3.2 and BRK1 proteins each contain a BUB1-MAD3 N-terminal conserved domain organised into a tetratricopeptide motif repeat (TPR) (Bolanos-Garcia *et al.*, 2009). BRK1 contains a C-terminal protein kinase domain, which is absent from MAD3.2, as in BUBR1/MAD3.1 (Fig. 2a, Supporting Information Fig. S1). BRK1 displays 49% and 61% identity over its entire length with the recently characterized BRK1 from monocots (*Oryza sativa*) and dicots (*Vitis vinifera*), respectively (Karpov *et al.*, 2010; Wang *et al.*, 2012) (Fig. S2a). The spatial folding of plant BRK1 and human BUB1 kinase domains display a high degree of similarity (Fig. S2b). We found that MAP65-3 interacted with BUB3.1, MAD2, BUBR1/MAD3.1, MAD3.2 and BRK1 in yeast. In addition to the previously described interaction between BUB3.1, BUBR1/MAD3.1 and MAD2 (Caillaud *et al.*, 2009), we confirmed that all SAC subunits interacted with each other in Y2H screening, indicating that they form a complex (Fig. 2b). Except for the interaction between BUBR1/MAD3.1 and MAD2, which was not detected when BUBR1/MAD3.1 was used as bait, all these interactions were confirmed in a reciprocal bait–prey experiment.

MAD3.1 interacts specifically with MAD3.2 and MAD2 at chromocentres *in planta*

We investigated whether and where the interactions between SAC subunits occurred *in planta*, by bimolecular fluorescence complementation (BiFC) analysis. Following transient expression in *N. benthamiana* leaf epidermis, MAP65-3 fused to GFP was found associated with large bundles of cortical MT arrays (Fig. 2c). BRK1 and MAD3.2 with GFP fused to the N- or C-terminus were detected in both the nucleus and the cytoplasm (Fig. S3), as previously described for MAD2 and BUB3.1, whereas BUBR1/MAD3.1 was specifically targeted to the nucleus (Caillaud *et al.*, 2009). We showed, by BiFC, that the co-expression of constructs encoding MAP65-3:YC (MAP65-3 fused to the C-terminal half of YFP) and BUB3.1:YN (BUB3 fused to the N-terminal half of YFP) resulted in the targeting of the reconstituted YFP complexes to MT arrays ($n = 20$; Fig. 2d). Similar results were obtained with all the SAC components tested, except for BRK1, for which no YFP fluorescence was detected (Fig. S3). We previously reported that BUBR1/MAD3.1 and MAD2 interact specifically at chromocentres in the interphasic nuclei (Caillaud *et al.*, 2009). In contrast to the homogeneous distribution of BUBR1/MAD3.1 and MAD3.2 within nucleoplasm, the interactions between MAD3.1:YN and MAD3.2:YC were observed exclusively as bright subnuclear foci (Fig. 2d). Using the centromeric histone H3 (CENH3) variant from Arabidopsis GFP:HTR12 as an *in vivo* marker for centromeres (Talbert *et al.*, 2002; Lermontova *et al.*, 2011), we confirmed that BUBR1/MAD3.1 and MAD3.2 interacted specifically at interphase centromeres, corresponding to the chromosomal position at which kinetochore proteins associate (Fig. 2d). By contrast, MAD3.2 interacted with MAD2 or BUB3.1 in the nuclei and cytoplasm of epidermal cells (Fig. S3).

BUBR1/MAD3-encoded genes are co-expressed with *MAP65-3* in dividing cells and nematode feeding cells

In our previous studies, we showed that the *MAP65-3*, and *BUBR1/MAD3.1* promoters drove expression in tissues enriched in dividing cells (Caillaud *et al.*, 2009). We investigated during plant development the pattern of expression of the newly identified SAC complex genes, *MAD3.1* and *BRK1*, in *A. thaliana* transgenic lines ($n = 5$) transformed with the corresponding promoter-GUS reporter gene constructs. Pro*MAD3.2*:GUS directed expression early in organ development, in tissues with a high proportion of dividing cells, such as young leaves (Fig. 3a), root meristems (Fig. 3b) and lateral root primordia (Fig. 3c). Pro*MAD3.2*:GUS expression was also observed in the carpels of floral buds and flowers (Fig. 3d,e) and in the leaf vascular bundles (Fig. 3f). In Pro*BRK1*:GUS lines, GUS expression was observed in young leaves but not in root meristems (Fig. 3h–j). In flowers, *BRK1* expression was detected in the papillae and pollen (Fig. 3k,l,n). This pattern of expression suggests a role for this gene in the development of aerial organs. Thus, *BUBR1/MAD3.1* and *MAD3.2* are co-expressed with *MAP65-3* in all dividing plant cells, whereas *BRK1* gene function may be restricted to the shoot.

We then investigated whether SAC components were induced in response to nematode attack, as reported for *MAP65-3* (Caillaud *et al.*, 2008). Studies of the root-knot nematode infection of promoter-GUS transgenic lines showed that the *BUB3.1,*

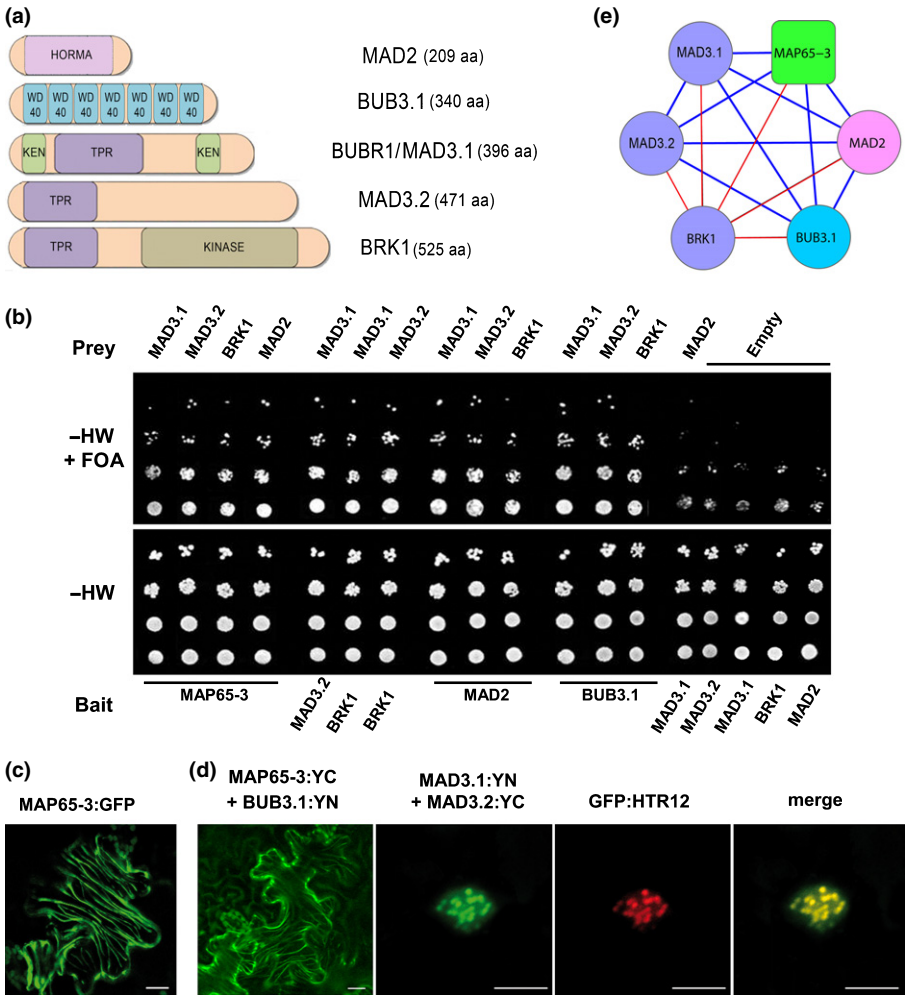

Fig. 2 Interactions between the core components of the spindle assembly checkpoint (SAC) and MAP65-3 in yeast and *in planta*. (a) Domain organisation of Arabidopsis MAD2, BUB3.1, BUBR1/MAD3.1, MAD3.2 and BRK1. The conserved functional motifs – KEN, tetratricopeptides repeat motif (TPR), kinase, WD-40 repeats and HORMA (PF02301) domain – are indicated. Proteins are drawn to scale. (b) Interactions in the yeast two-hybrid (Y2H) split-ubiquitin system. Dilution series of yeast JD53 cells expressing both bait:Cub:URA3 fusions and Nub:prey fusions were grown on yeast medium minus histidine and tryptophan (-HT) but containing 5-fluoroorotic acid (5-FOA), as indicated. Interaction resulted in uracil auxotrophy and 5-FOA resistance. (c) MAP65-3:GFP expression in agroinfiltrated tobacco (*Nicotiana benthamiana*) epidermal leaf cells. (d) *In planta* bimolecular fluorescence complementation (BiFC) assay. Confocal images of agroinfiltrated tobacco epidermal leaf cells co-expressing the prey or bait fused to the N- and C-terminal halves of the YFP (YN and YC, respectively) (green channel), and GFP:HTR12 (red channel). The merged image shows that BUBR1/MAD3.1 and MAD3.2 interaction colocalised with HTR12 in the yellow chromocentre spots. Bars, 10 μm. (e) Interaction network. Edge colours indicate the type of assay detecting the interaction for each pair: Y2H (red) or both BiFC and Y2H (blue).

BUBR1/MAD3.1, *MAD3.2* and *MAD2* genes were expressed in galls at early stages of giant cell formation, corresponding to nuclear division, < 48 h after giant cell initiation, 3 dpi (Fig. 4). Intriguingly, although no *BRK1* expression was observed in dividing root cells, weak GUS expression was observed in galls 10 dpi in Pro*BRK1*:GUS lines, suggesting that *BRK1* expression may be transiently activated in response to nematode attack. For up to 3 wk, during the period of giant cell formation, a similar pattern of expression was observed for all SAC subunits (3–21 dpi). The upregulation of expression for these genes was confirmed by RT-qPCR analysis (Fig. S4). Sections through galls showed GUS staining in developing giant cells and in the surrounding dividing cells (Fig. 4). No GUS activity was detected in the cortical cells of the gall. Overall, these results show that SAC genes are co-expressed with *MAP65-3* in dividing cells and in the giant cells induced by the nematodes.

In Arabidopsis, BUBR1/MAD3.1 protein concentrates at the mitotic spindle during metaphase–anaphase transition whereas BRK1 localises on kinetochores

We investigated the spatial distribution of SAC proteins in Arabidopsis, upon stable expression of GFP fusions of SAC subunits genes. When expressed under their native promoters, GFP fusions were hardly detectable in Arabidopsis. We therefore used the *MAP65-3* promoter to drive mitosis-specific GFP fusions expression (Caillaud *et al.*, 2008). As expected, during normal mitosis (i.e. without the addition of mitotic drugs), MAD3.1:GFP and MAD3.2:GFP were not localised at the kinetochores (Fig. 5). By contrast, BRK1:GFP was detectable at kinetochores throughout mitosis (Fig. 5). To confirm this localisation, we first used crosses between $Pro_{MAP65\text{-}3}$:BRK1:YFP and Pro35S:HTR12:GFP. Imaging of *Arabidopsis* roots simultaneously expressing both the centromeric histone 3 variant fused to GFP (HTR12:GFP) and BRK1:YFP showed the colocalisation of BRK1 and HTR12 in spots in interphase nuclei as well as during mitosis (Fig. 6a). Moreover, we performed whole-mount immunolocalisation using anti-HTR12 specific antibodies (Talbert *et al.*, 2002) in BRK1:GFP plants (Fig. 6b). These experiments demonstrated the BRK1 localisation at interphase centromeres and on kinetochores during mitosis (Fig. 6b). Careful observation of the subcellular distribution of the SAC subunits during cell cycle progression revealed that there was a signal for MAD3.1:GFP, but not for MAD3.2:GFP, at the mitotic spindle (Fig. 5). Interestingly the fluorescence could not be detected in all the surrounding cells, indicating that these proteins were regulated by

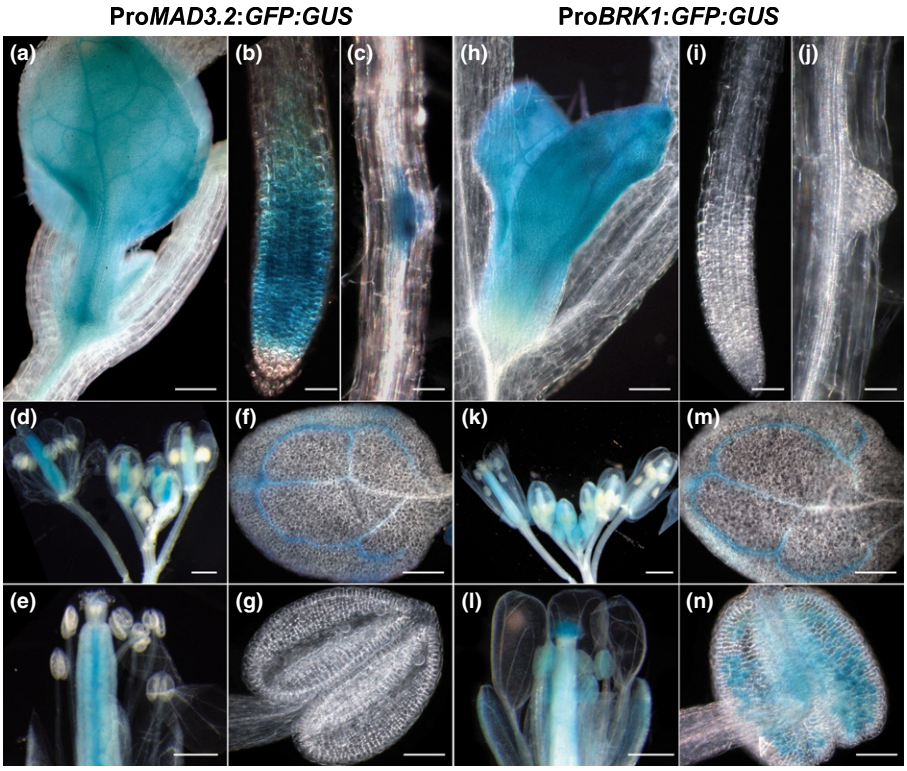

Fig. 3 Expression pattern of *MAD3.2* and *BRK1* during Arabidopsis development. Arabidopsis lines transformed with the promoter-GUS fusions *ProMAD3.2:GFP:GUS* (a–g) or *ProBRK1:GFP:GUS* (h–n). (a, h) Developing leaves of 7-d-old seedlings. (b, i) Root meristems. (c, j) Lateral root primordia. (d, k) Inflorescences. (e, l) Flowers. (f, m) Leaves. (g, n) Anthers. Bars: (a–c, e, f, h–j, l, m) 100 μm; (d, k) 200 μm; (g, n) 25 μm.

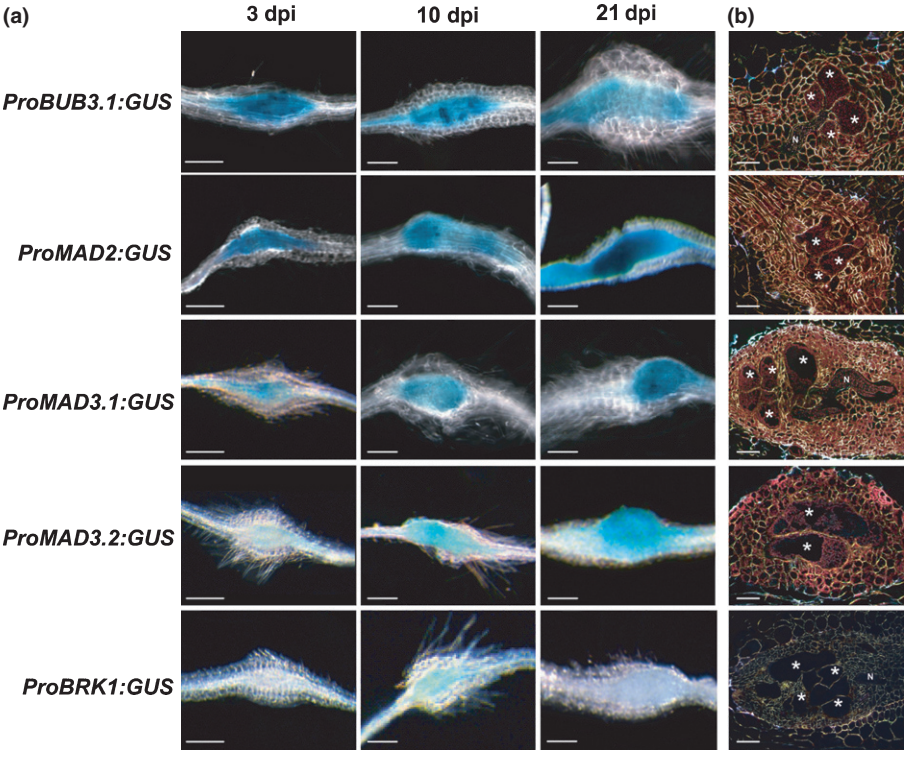

Fig. 4 Promoter-GUS fusions reveal the expression of the spindle assembly checkpoint (SAC) components in galls induced by root-knot nematodes. (a) GUS activity in root galls from 3 to 21 d after *Meloidogyne incognita* infection. (b) Section of 21 d post infection (dpi) galls examined by dark-field microscopy. GUS activity (detected by the formation of a pink precipitate) is observed (*) in the giant cells and (N) in the cells surrounding the giant cells and the nematode larvae. Bars: (a) 100 μm; (b) 25 μm.

both transcriptional and post-transcriptional mechanisms, as described for MAP65-3 (Caillaud *et al.*, 2008). We have shown that BUBR1/MAD3.1 localises to kinetochore MTs following MT-destabilising drug treatment (Caillaud *et al.*, 2009). Indeed, BiFC revealed that MAD3.1:YN localised to the MT network when coexpressed with MAP65-3:YC (Fig. S3), suggesting a particular role for BUBR1/MAD3.1 at the interface between the kinetochore and spindle MTs.

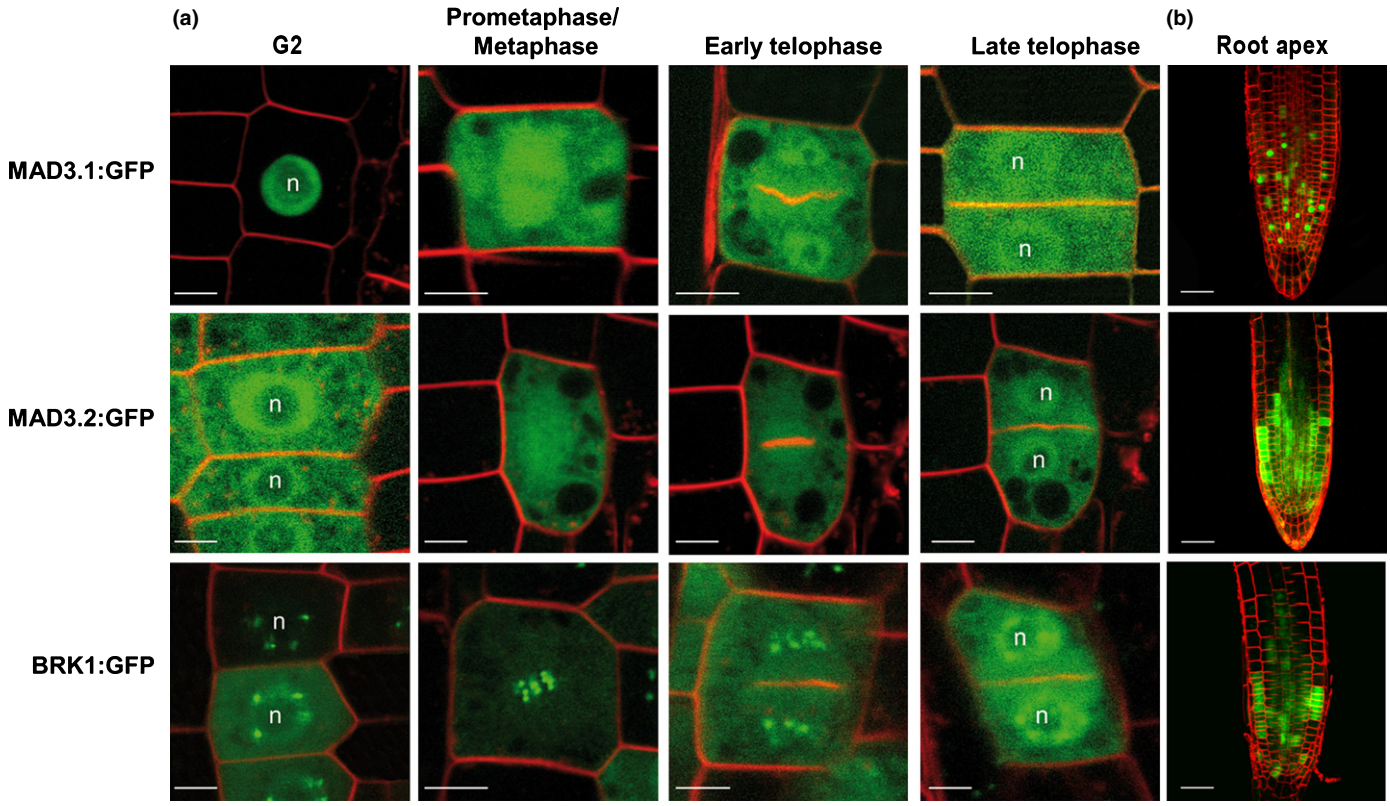

Fig. 5 Subcellular distribution of GFP fusions with spindle assembly checkpoint (SAC) components during mitosis in *Arabidopsis* roots. (a) Single optical sections of meristematic root cells expressing MAD3.1:GFP, MAD3.2:GFP or BRK1:GFP fusion constructs under the control of the MAP65-3 promoter (green channel). The plasma membrane was stained with FM4-64 (red channel). MAD3.1:GFP was detected in the cytoplasm, but gave a stronger signal at the mitotic spindle. BRK1:GFP was detected at the kinetochores of chromosomes throughout mitosis. n, nuclei. (b) Root apex showed GFP in restricted cells. Bars: (a) 5 μm; (b) 20 μm.

Mutations in the *BUBR1/MAD3.1* and *MAD3.2* genes impair root growth in response to treatment with MT-destabilising drugs

We then investigated the loss-of-function phenotypes of SAC subunits in Arabidopsis. In higher eukaryotes, homozygous null mutants of essential SAC components present early embryonic lethality (Basu *et al.*, 1999; Kitagawa & Rose, 1999; Dobles *et al.*, 2000; Kalitsis *et al.*, 2000). In plants, Arabidopsis *bub3.1* is lethal whereas rice *brk1* mutants are sterile (Lermontova *et al.*, 2008; Wang *et al.*, 2012). We identified T-DNA insertion mutations at the *BUBR1/MAD3.1, MAD3.2* and *BRK1* loci (Fig. 7a). In *brk1* mutant, the T-DNA integration took place into the twelfth intron and generated a premature stop codon. RT-PCR experiments confirmed that no full-length transcript was produced in the corresponding mutants (Fig. 7b). A truncated *brk1* transcript (exon1 to 12) was detected in *brk1* mutant and led to a deletion of 103 amino acids. This BRK1 truncated protein lacked the C-terminal part of the kinase domain. The *mad3.1*, *mad3.2* and *brk1* mutants were morphologically similar to wild-type plants under normal growth conditions and developed normal roots, leaves, shoot and flowers (Fig. S5). In parallel, we generated double *mad3.1 brk1*, *mad3.1 mad3.2, mad3.2 brk1* and triple *mad3.1 mad3.2 brk1* mutants to determine whether the lack of a developmental phenotype was due to redundancy.

We first investigated whether knock-outs of genes from the BUB1-BUBR1/MAD3 family impaired the progression of mitosis following treatment with MT-destabilising drugs. The addition of oryzalin to the growth medium inhibited the root growth of the two single mutants (*mad3.1* and *mad3.2*) and of the double *mad3.1 brk1*, *mad3.1 mad3.2, mad3.2 brk1* and the triple mutants (Fig. 7c), but not that of *brk1*. The phenotype of the double and triple mutants was statistically indistinguishable from either *mad3.1* or *mad3.2* parent, suggesting that the two genes act at the same pathway. This growth phenotype is consistent with a defect in the arrest of the cell cycle in metaphase to repair the lesions, as initially described for *bub* mutants in *S. cerevisiae* (Hoyt *et al.*, 1991). Thus, BUBR1/MAD3.1 and MAD3.2 are important for mitosis arrest in the occurrence of defects in the root, whereas BRK1 may play a tissue-specific role in the aerial organs of the plant.

We then investigated the ability of root-knot nematodes to induce their giant feeding cells in single mutants and in the double and triple (*mad3.1 mad3.2 brk1*) mutants. Following nematode infection, all mutants had numbers of galls and egg masses similar to those observed in the corresponding wild-type plants (Fig. S6). Thus, nematodes were able to infect the plants and

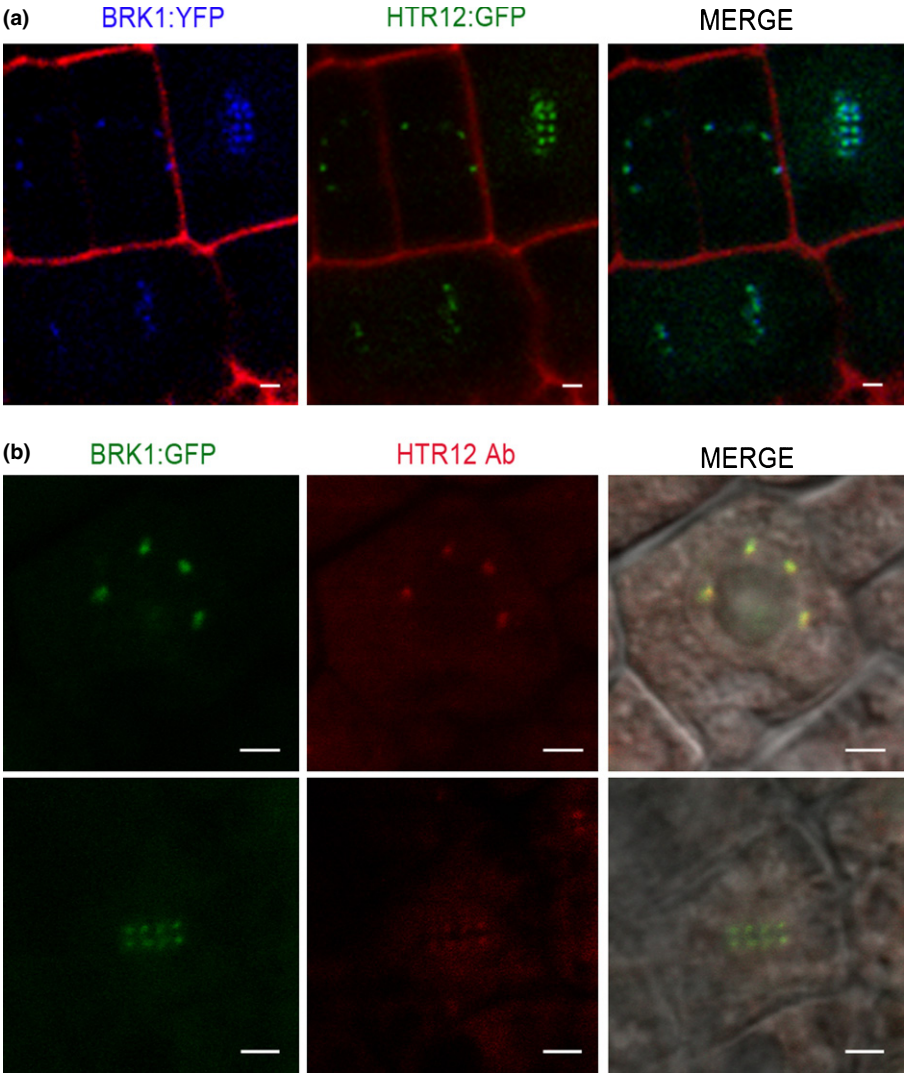

Fig. 6 BRK1 colocalises with the centromeric histone 3 variant HTR12 in interphase centromeres and in the kinetochores during mitosis in Arabidopsis. (a) Optical sections of root cells expressing BRK1:YFP (blue channel) and HTR12:GFP (green channel). The plasma membrane was stained with propidium iodide (red channel). The merged image shows BRK1 and HTR12 colocalisation in spots corresponding to the centromeres. (b) Whole-mount immunolocalisation using anti-HTR12 specific antibodies and Alexa Fluor 594 secondary antibodies (red channel) in BRK1:GFP (green channel) plants during interphase (above) or mitosis (below). The merged image shows BRK1 and HTR12 colocalisation in yellow. Bars, 2 μm.

induce a functional feeding site for their development and reproduction.

Losses of function for *mad3.1*, *mad 3.2* and *brk1* result in defects during mitosis

For analyses of chromosome segregation in the absence of functional BUBR1/MAD3 and BRK1 proteins, we introgressed the H2B:YFP fluorescent marker into *mad3.1*, *mad3.2* and *brk1* single, double or triple mutants. We then carried out *in vivo* confocal microscopy to analyse chromosome rearrangements in the various mutants during mitosis. We detected misaligned chromosomes on the metaphase plate in the *mad3.1* mutant (8% of divisions, number of analysed mitotic figures $n = 70$, $P < 0.05$, Fig. 8a), resulting in the presence of lagging chromosomes in anaphase (Fig. 8b). No obvious mitosis defect was observed in *mad3.2* and *brk1* single and double mutants in the root meristem cells (Fig. 8c–h). Interestingly, the *mad3.1 mad3.2* double mutant had a stronger phenotype, with lagging chromosomes in anaphase (21% of divisions, number of analysed mitotic figures $n = 58$, Fig. 8i–k,m–p), which may result in the formation of micronuclei in late telophase (Fig. 8l,l′). As observed for the *mad3.1 mad3.2* mutant, the *mad3.1 mad3.2 brk1* triple mutant displayed slow chromosome congression and an unstable metaphase plate (Fig. 8q–r). This considerably delayed anaphase and chromosome segregation, leading in some cases to chromosome lagging and unequal separation of chromosomes during mitosis (Fig. 8q–r). Interestingly, chromosome mis-segregations were also observed in the shoot apical meristem dividing cells of *brk1* mutant (16% of divisions, number of analysed mitotic figures $n = 50$, $P < 0.05$, Fig. 8s,t). Thus, BUBR1/MAD3.1, MAD3.2 and BRK1 are important for correct chromosomes alignment during the transition between metaphase and anaphase. Finally, to visualise the dynamics of the MT network during the cell division in the *mad3.1 mad3.2* mutants, we introgressed the MT fluorescent marker MBD:GFP into mutants already expressing H2B:YFP. *In vivo* cell imaging of dividing cells in the root meristem revealed major cytoskeletal abnormalities. After nuclear envelope breakdown, defects in spindle polarity and spindle MT organisation occurred in *mad3.1 mad3.2* mutants (Fig. 8i–k,m–o). Time-lapse

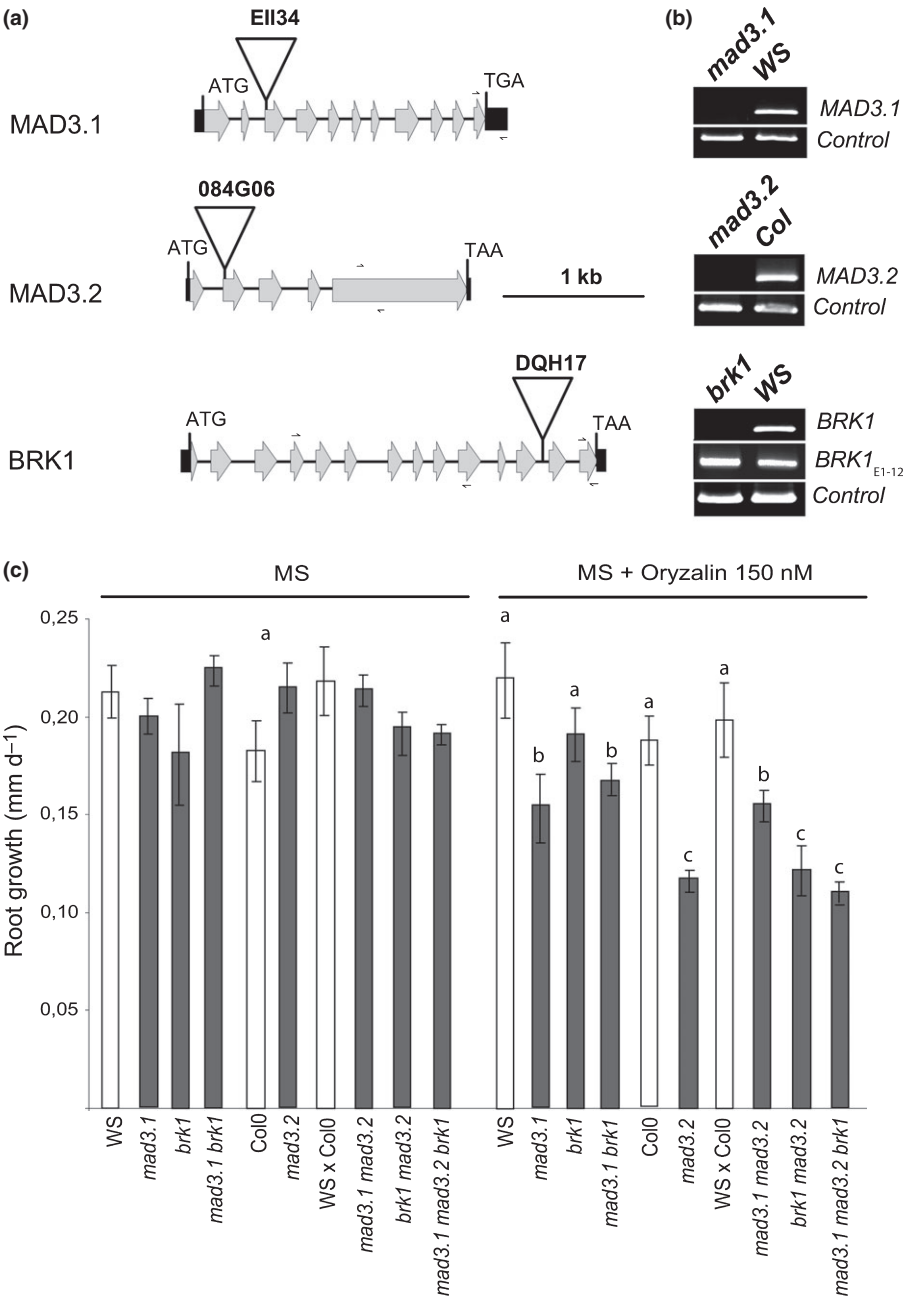

Fig. 7 Phenotype of *mad3.1*, *mad3.2* and *brk1* single, double and triple mutant plants. (a) Schematic illustration of the genomic organisation of the *BUBR1/MAD3.1*, *MAD3.2* and *BRK1* genes and the positions of the corresponding T-DNA insertions. Exons, introns and untranslated regions are displayed as open arrows, lines and shades boxes, respectively. Primers used in QPCR analyses are indicated. (b) RT-PCR showing that transcripts of these genes were present in the wild-type Arabidopsis ecotypes Col and WS. Amplicons spanning the insertion sites were absent from all KO mutants. A truncated *BRK1* transcript (exon1 to 12; E1–12) was detected in the *brk1* mutant. The MAP65-3 CDS was used as a positive control. (c) Root growth of 25-d-old mutants (grey bars) or wild types (white bars, WS, Col0 or WS/Col0) seedlings grown on vertically orientated placed plates in the presence and absence of 150 nM oryzalin. The data shown are means (± SD) of > 25 seedlings, for experiments carried out in triplicate. The significance of differences between the values was assessed in Student's *t*-test. Data with the same letter are not statistically different ($P < 0.01$).

analysis revealed the presence of tilted phragmoplasts in *mad3.1 mad3.2* (Fig. S7); such asymmetrical growth of the phragmoplast often led to the formation of micronuclei (Fig. 8l,l′). Thus, BUBR1/MAD3.1, MAD3.2 and BRK1 play a key role in ensuring the fidelity of chromosome segregation during mitosis.

Discussion

The SAC is responsible for ensuring the fidelity of chromosome segregation during cell division. Animal and fungal SAC components have been studied in detail, but the role of these components remains to be determined in plants. We report here an analysis of the function of plant SAC components in mitosis demonstrating the essential role of the two BUBR1/MAD3-related proteins for accurate mitosis in Arabidopsis.

Two BUBR/MAD3-related proteins and one BUB1-related kinase are components of the plant SAC and interact with MAP65-3

We identified two new SAC members in Arabidopsis, MAD3.2 and BRK1, and showed that they interacted physically with the characterised proteins BUBR1/MAD3.1, MAD2 and BUB3.1. These results confirm that all these SAC subunits interact with each other as part of a protein complex. The failure to confirm a direct interaction between BRK1 and the other proteins by BiFC

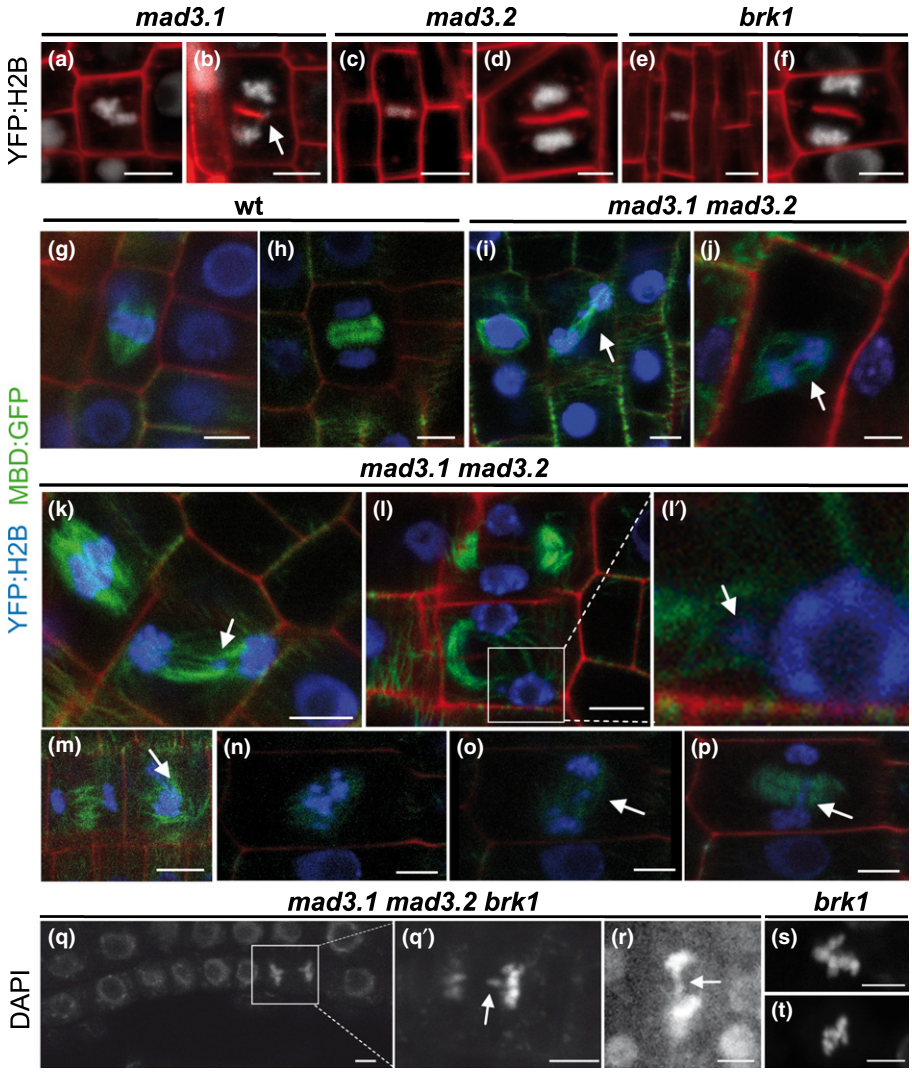

Fig. 8 Mitotic defects in single *bubr1/mad3.1, brk1*, double *bubr1 bub1.2* and triple *bubr1 bub1.2 brk1* mutants. (a–p) Single optical sections of meristematic root cells expressing H2B:YFP (blue or white channel) and (g–p) MBD:GFP (green channel). The plasma membrane was stained with (a–f) FM4-64 or (g–p) propidium iodide (red channel). (a, b) The *mad3.1* single mutant showed defects in chromosome alignment during metaphase (a) and consequent lagging chromosomes in telophase (b, arrow). The *mad3.2* (c, d) and *brk1* (e, f) single mutants have a phenotype similar to that of the WT during metaphase (c, e) and telophase (d, f) in root meristems. (g, h) Wild-type mitosis with metaphasic spindle (g) and phragmoplast (h). (i–p) The *mad3.1 mad3.2* double mutant presented mitotic spindle defects, with an oblique spindle (i–k), or a tripolar spindle in some cases (j, m, n). This mutant presented lagging chromosomes (i–k, n–p) and the subsequent formation of micronuclei (l, l′ (arrow)). (l) A selected frame from a time-lapse analysis presented in Supporting Information Fig. S7. (q–r) DAPI-stained cells of the *mad3.1 mad3.2 brk1* triple mutant showed defects similar to those of the *mad3.1 mad3.2* double mutant. (q, q′) Chromosome misalignment. (r) Anaphase bridge. (s, t) Chromosome misalignments in *brk1* DAPI-stained shoot apical meristem cells. Bars, 5 μm.

are probably due to the BRK1 subcellular mislocalisation in non-dividing tobacco epidermal cells. Indeed, Arabidopsis BRK1 was not detected in kinetochores in these cells as reported in Arabidopsis, but in the nucleus and the cytoplasm. The high-throughput generation of core cell cycle binary protein–protein interaction network using Y2H and BiFC revealed that these two interaction assays are complementary (Boruc *et al.*, 2010). Using a positive reference set of 64 known pairwise Arabidopsis core cell cycles, only 44% were detected by both BiFC and Y2H. Focusing on 77 pairwise interactions detected by Y2H, 16 were not confirmed by BiFC (Boruc *et al.*, 2010). The Arabidopsis BUBR1/MAD3.1 and MAD3.2 proteins resemble the MAD3 proteins of yeasts, but they differ from BRK1s and vertebrate BUB1s and BUBR1s in that they lack a C-terminal kinase domain. The Arabidopsis and rice BRK1s have identical structures and the highly conserved kinase domain has been shown to be possess Ser/Thr kinase activity in rice (Wang *et al.*, 2012). MAD3.2 also lacks the conserved KEN boxes critical for checkpoint activity (Sczaniecka *et al.*, 2008). BRK1, BUBR1/MAD3.1 and MAD3.2 each contain a conserved N-terminal BUB1-MAD3 domain including the tetratricopeptide repeat motif (TPR) known to mediate binding to the kinetochore MT-binding protein Blinkin (KNL1/Spc105/CASC5) (Kiyomitsu *et al.*, 2007; Bolanos-Garcia *et al.*, 2009). Blinkin connects BUB1 and BUBR1 with the hMis12, Ndc80 and Zwint-1 complexes (Kiyomitsu *et al.*, 2011). These SAC components interact with the MT bundler MAP65-3. The interaction between MAP65-3 and BUB3.1 has been confirmed biochemically in cell culture, by tandem affinity purification coupled to mass spectrometry, using BUB3.1 as a bait (Van Leene *et al.*, 2010). This interaction is also consistent with the interactions of SAC components with MAP65 homologues playing key roles in the organisation of central spindles and midzone formation in yeast (Ase1p, (Daniel *et al.*, 2006)) and humans (PRC1, (Kurasawa *et al.*, 2004)). Interestingly, Ase1p was recently identified as an essential regulator of metaphase spindle length and chromosome segregation by its major contribution to the outward-pushing force generated by spindle MTs (Syrovatkina *et al.*, 2013).

Despite their extensive similarities in terms of sequence and domain architecture, BUBR1/MAD3 and BUB1 play different roles in the SAC (Bolanos-Garcia *et al.*, 2009). Animal and fungal species with BUB family genes generally produce one or two BUB-like proteins, usually one BUB1 and one BUBR1 or

MAD3 protein. These paralogous pairs arose from independent gene duplications during evolution, followed by parallel subfunction partitioning in which the conservation of the ancestral, amino-terminal KEN box and that of (pseudo) kinase activity were mutually exclusive (Suijkerbuijk *et al.*, 2012). We showed that monocot (rice) and dicot (Arabidopsis) plants contained three BUB1/BUBR1/MAD3 proteins, including two MAD3 and one BUB1-related protein retaining a kinase domain (BRK1).

BUBR1/MAD3.1 and MAD3.2 are encoded by cell cycle-regulated genes and are able to interact specifically at centromeres *in planta*

Promoter-GUS fusions showed that *BUBR1*/*MAD3.1*, *MAD3.2*, *MAD2* and *BUB3.1* were co-expressed with *MAP65-3* in all dividing cells (Caillaud *et al.*, 2009; this study) and in giant cells induced by nematodes. The activity of *BRK1* promoter was not detected in root meristems suggesting a specific BRK1 role in shoot dividing cells accordingly with the mitotic defects observed in *brk1*. Even though we did not observe obvious mitotic defects in *brk1* root meristems, we cannot exclude the expression of *BRK1* in the root meristem. Indeed, the absence of GUS staining in root meristems may reflect the requirement of additional elements possibly present in *BRK1* intragenic regions as described for *CENH3* (Heckmann *et al.*, 2011). In addition to the previously described interactions between BUB3.1, BUBR1/MAD3.1 and MAD2 (Caillaud *et al.*, 2009), we showed that MAD3.2, like MAD2, was able to interact specifically with BUBR1/MAD3.1 at interphase centromeres. Kinetochore protein loading occurs at the centromeres during mitosis. An essential event in centromere specification was recently revealed by characterisation of the role of Arabidopsis KINETOCHORE NULL2 (KNL2) protein in CENH3 loading (Lermontova *et al.*, 2013).

We previously showed that the BUBR1/MAD3.1, BUB3.1 and MAD2 proteins were recruited to the kinetochore only in cases of damage during spindle assembly in tobacco cell cultures (Caillaud *et al.*, 2009). During normal mitosis in Arabidopsis, no GFP signals, except for BRK1:GFP, were detected at the kinetochores. BRK1 was found associated with centromeres in G2 and on kinetochores throughout the mitotic cell cycle, as also observed in immunolocalisation studies in rice (Wang *et al.*, 2012). The absence of a KEN box motif may account for the persistence of BRK1 on the kinetochore. Before entry into G2 during mitosis, the G2, BUB3.1, MAD3.2 and MAD2 proteins were localised in the nucleus, giving only a weak cytoplasmic signal, whereas MAD3.1 was found exclusively in the nuclei. No kinetochore recruitment was observed during prometaphase and metaphase during normal mitosis. A kinetochore localisation of the SAC during prometaphase is a common characteristic of higher eukaryotes (Wei *et al.*, 2011), but it is difficult to observe under physiological conditions in *S. cerevisiae*, and alterations or defects of the kinetochore or spindle integrity are required for clear enrichment of the kinetochore in SAC proteins (Kerscher *et al.*, 2003). Rapid protein turnover at the kinetochore prevents imaging by confocal microscopy. Our data suggest that plant kinetochores do not recruit large amounts of these SAC proteins during normal mitosis, consistent with the early link between chromosomes, MTs and spindle formation, which begins outside of the nucleus, before nuclear envelope breakdown, in plants (Vos *et al.*, 2008). BUBR1/MAD3.1 and BUB3.1 were found at a higher concentration at the mitotic spindle, suggesting a potential translocation from kinetochores to spindle poles along MTs, as reported for human MAD2 (Howell *et al.*, 2000).

Losses of function for *mad3.1* and *mad3.2*, or *brk1* result in defects during mitosis

We investigated the role of these proteins in plants, by characterising the *mad3.1*, *mad3.2* and *brk1* single, double and triple mutants. No sterility resembling the defect of rice *brk1* mutants was observed (Wang *et al.*, 2012). This sterility phenotype in rice is caused by the early separation of sister chromatids after metaphase I. Despite their normal growth and development, all the mutants other than *brk1* were highly sensitive to the MT-destabilising agent oryzalin. The lack of mitosis arrest, whereas all chromosomes have not properly attached to the spindle apparatus, will lead to unequal repartition of the genetic material. Generation of daughter cells with fewer or greater number of chromosomes, may lead to cell death, or cell division defects. Arabidopsis mutants, for example *clasp,* that are hypersensitive to MT-destabilizing drugs was reported as affected in cell division and expansion (Ambrose *et al.*, 2007). Thus, as in *S. cerevisiae*, the plant SAC is required to arrest cell division only when the structure of the spindle is disrupted, and is therefore not required under normal growth conditions (Hoyt *et al.*, 1991; Li & Murray, 1991). In higher eukaryotes, homozygous null mutants for essential SAC components present early embryonic lethality (Basu *et al.*, 1999; Kitagawa & Rose, 1999; Dobles *et al.*, 2000; Kalitsis *et al.*, 2000). The lack of lethality observed in Arabidopsis may be due to the high degree of plasticity of plant development and/or genetic redundancy. The elimination of the two BUBR1/MAD3 proteins led to typical mitotic defects, with metaphase chromosomes failing to congress and align correctly, leading to lagging chromosomes and the formation of micronuclei. In giant cells, the polyploidisation (Huang & Maggenti, 1969) may also allow bypass of the mutant phenotype. Thus, as demonstrated for MAD3 and BUBR1 in yeasts, worms and higher eukaryotes (Musacchio & Salmon, 2007), our results suggest that plant BUBR1/MAD3s play a key role in ensuring chromosomal stability.

The SAC detects incorrect kinetochore–spindle linkages and delays the onset of anaphase until correct attachments have been established, by restricting the activity of the E3 ubiquitin ligase APC/C with key mitotic substrates, thereby preventing premature sister chromatid separation and exit from mitosis. Like MAD2, BUBR1/MAD3 binds directly to and inhibits CDC20, the essential cofactor of APC/C. MAD3 and BUBR1 also determines basal mitotic timing, the minimum time elapsed between nuclear envelope breakdown (NEB) and anaphase onset (Meraldi *et al.*, 2004). MAD3 and BUBR1 also function to promote proper kinetochore-MT linkage (Lampson & Kapoor, 2005). The multifunctionality of the MAD3 and BUBR1 proteins

renders the phenotypes resulting from their inactivation lethal in all other metazoans except in *Drosophila melanogaster* (Buffin *et al.*, 2007). The chromosome delay and unstable metaphase alignment seen in the *mad3.1 mad3.2* or *brk1* mutant is consistent with these proteins playing an important role in the promotion of kinetochore-MT attachment, as reported in mammalian cells after siRNA treatment (Lampson & Kapoor, 2005). The cytoskeletal abnormalities, with defects of spindle polarity and spindle MT organisation, detected may be a consequence of defective kinetochore-MT attachment or, more specifically, alterations to the activities of kinetochore-associated factors influencing MT stability or dynamics. Similar defects have been reported only in *D. melanogaster*, and the depletion of fly proteins that bind to and stabilise MT^{+} ends, such as CLASP and EB1, results in shortened spindles and congressional problems (Rahmani *et al.*, 2009). In plants, the coordinated activities of specific structural and motor MAPs and the gamma tubulin complex, associated with post-translational modifications of spindle-associated proteins, are also essential for robust spindle function (Janski *et al.*, 2012). Such proteins, including MAP65-3 in particular, are thus potential candidates for a role in BUBR1/MAD3 regulation. Even though the three BUB1 and BUBR1/MAD3 proteins are not essential for giant cell ontogenesis, the study of their dynamics during the multiple and synchronous nuclear divisions induced by root-knot nematodes may represent an original contribution to the study of the SAC functioning in multinucleate cells.

Together, our data provide clues as to the role of SAC in ensuring that mitosis occurs correctly in plants. As in yeast and *Drosophila*, the SAC mechanism in plants is not essential to organism survival in general, probably coming into play only when the structure of the spindle is disrupted. Defects of chromosome structure and number are lethal in all animals, but plants have evolved remarkable adaptability and plasticity, enabling them to bypass these defects.

Acknowledgements

We thank Marylin Vantard (iRTSV, Grenoble, France), Anne-Catherine Schmit (IBMP, Strasbourg, France), Ariane Abrieu and Anna Castro (CRBM, Montpellier, France) and Paulo Vieira (Evora University, Evora, Portugal) for fruitful discussions. We thank the Microscopy Platform-Sophia Agrobiotech Institut-INRA 1355-UNS-CNRS 7254- INRA PACA-Sophia Antipolis for access to instruments and technical advices. We thank Richard Cyr (Pennsylvania State University, PA, USA) for generously providing us with *Pro$_{35S}$:MBD:GFP* seeds, Steve Henikoff for generously providing us with HTR12 antibodies and Frédéric Berger (Temasek LifeSciences Laboratory, Singapore) for *Pro$_{35S}$:H2B:YFP* and *Pro$_{35S}$:HTR12:GFP* seeds, Catherine Mura for growing tobacco plants, Mansour Karimi (VIB Ghent, Belgium) for the plant Gateway vectors, and Imre E. Somssich (Max-Planck Institut, Köln, Germany) for the split-ubiquitin system. This work was funded by INRA and by the French Government (National Research Agency, ANR) through the ANR-08-GENM-014 'SCRIPS' and 'Investments for the Future' LABEX SIGNALIFE: program reference # ANR-11-LABX-0028-01. L.P. was supported by a fellowship from the Ministère de la Recherche et l'Enseignement Supérieure.

References

Ambrose JC, Shoji T, Kotzer AM, Pighin JA, Wasteneys GO. 2007. The *Arabidopsis CLASP* gene encodes a microtubule-associated protein involved in cell expansion and division. *Plant Cell* **19**: 2763–2775.

Basu J, Bousbaa H, Logarinho E, Li Z, Williams BC, Lopes C, Sunkel CE, Goldberg ML. 1999. Mutations in the essential spindle checkpoint gene *bub1* cause chromosome missegregation and fail to block apoptosis in *Drosophila*. *The Journal of Cell Biology* **146**: 13–28.

Bolanos-Garcia VM, Kiyomitsu T, D'Arcy S, Chirgadze DY, Grossmann JG, Matak-Vinkovic D, Venkitaraman AR, Yanagida M, Robinson CV, Blundell TL. 2009. The crystal structure of the N-terminal region of BUB1 provides insight into the mechanism of BUB1 recruitment to kinetochores. *Structure* **17**: 105–116.

Boruc J, Van den Daele H, Hollunder J, Rombauts S, Mylle E, Hilson P, Inzé D, De Veylder L, Russinova E. 2010. Functional modules in the *Arabidopsis* core cell cycle binary protein–protein interaction network. *Plant Cell* **22**: 1264–1280.

Buffin E, Emre D, Karess RE. 2007. Flies without a spindle checkpoint. *Nature Cell Biology* **9**: 565–572.

Caillaud M-C, Lecomte P, Jammes F, Quentin M, Pagnotta S, Andrio E, de Almeida Engler J, Marfaing N, Gounon P, Abad P *et al.* 2008. MAP65-3 microtubule-associated protein is essential for nematode-induced giant cell ontogenesis in *Arabidopsis*. *Plant Cell* **20**: 423–437.

Caillaud M-C, Paganelli L, Lecomte P, Deslandes L, Quentin M, Pecrix Y, Le Bris M, Marfaing N, Abad P, Favery B. 2009. Spindle assembly checkpoint protein dynamics reveal conserved and unsuspected roles in plant cell division. *PLoS ONE* **4**: e6757.

Chen RH, Waters JC, Salmon ED, Murray AW. 1996. Association of spindle assembly checkpoint component XMAD2 with unattached kinetochores. *Science* **274**: 242–246.

Cleveland DW, Mao Y, Sullivan KF. 2003. Centromeres and kinetochores: from epigenetics to mitotic checkpoint signaling. *Cell* **112**: 407–421.

Daniel JA, Keyes BE, Ng YPY, Freeman CO, Burke DJ. 2006. Diverse functions of spindle assembly checkpoint genes in *Saccharomyces cerevisiae*. *Genetics* **172**: 53–65.

De Almeida Engler J, Engler G, Gheysen G. 2011. Unreavelling the plant cell cycle in nematode induced feeding sites. In: Jones J, Gheysen G, Fenoll C, eds. *Genomics and molecular genetics of plant–nematode interactions*. Dordrecht, the Netherlands: Springer, 320–368.

De Almeida-Engler J, Favery B. 2011. The plant cytoskeleton remodelling in nematode induced feeding sites. In: Jones J, Gheysen G, Fenoll C, eds. *Exploiting genomics to understand plant–nematode interactions*. Dordrecht, the Netherlands: Springer, 369–393.

Dobles M, Liberal V, Scott ML, Benezra R, Sorger PK. 2000. Chromosome missegregation and apoptosis in mice lacking the mitotic checkpoint protein Mad2. *Cell* **101**: 635–645.

Heckmann S, Lermontova I, Berckmans B, De Veylder L, Baumlein H, Schubert I. 2011. The E2F transcription factor family regulates *CENH3* expression in *Arabidopsis thaliana*. *Plant Journal* **68**: 646–656.

Ho C-MK, Lee Y-RJ, Kiyama LD, Dinesh-Kumar SP, Liu B. 2012. *Arabidopsis* microtubule-associated protein MAP65-3 cross-links antiparallel microtubules toward their plus ends in the phragmoplast via its distinct C-terminal microtubule binding domain. *Plant Cell* **24**: 2071–2085.

Houben A, Schubert I. 2003. DNA and proteins of plant centromeres. *Current Opinion in Plant Biology* **6**: 554–560.

Howell BJ, Hoffman DB, Fang G, Murray AW, Salmon ED. 2000. Visualization of Mad2 dynamics at kinetochores, along spindle fibers, and at spindle poles in living cells. *The Journal of Cell Biology* **150**: 1233–1250.

Howell BJ, Moree B, Farrar EM, Stewart S, Fang G, Salmon ED. 2004. Spindle checkpoint protein dynamics at kinetochores in living cells. *Current Biology* **14**: 953–964.

Hoyt MA, Totis L, Roberts BT. 1991. *S. cerevisiae* genes required for cell cycle arrest in response to loss of microtubule function. *Cell* **66**: 507–517.

Huang C, Maggenti AR. 1969. Mitotic aberrations and nuclear changes of developing giant cells in *Vicia faba* caused by root-knot nematode, *Meloidogyne javanica*. *Phytopathology* **59**: 447–455.

Hussey PJ, Hawkins TJ, Igarashi H, Kaloriti D, Smertenko A. 2002. The plant cytoskeleton: recent advances in the study of the plant microtubule-associated proteins MAP-65, MAP-190 and the *Xenopus* MAP215-like protein, MOR1. *Plant Molecular Biology* **50**: 915–924.

Jammes F, Lecomte P, de Almeida-Engler J, Bitton F, Martin-Magniette M-L, Renou JP, Abad P, Favery B. 2005. Genome-wide expression profiling of the host response to root-knot nematode infection in *Arabidopsis*. *Plant Journal* **44**: 447–458.

Janski N, Masoud K, Batzenschlager M, Herzog E, Evrard J-L, Houlné G, Bourge M, Chabouté M-E, Schmit A-C. 2012. The GCP3-interacting proteins GIP1 and GIP2 are required for γ-tubulin complex protein localization, spindle integrity, and chromosomal stability. *Plant Cell* **24**: 1171–1187.

Kalitsis P, Earle E, Fowler KJ, Choo KHA. 2000. *Bub3* gene disruption in mice reveals essential mitotic spindle checkpoint function during early embryogenesis. *Genes & Development* **14**: 2277–2282.

Karimi M, Inzé D, Depicker A. 2002. GATEWAY™ vectors for *Agrobacterium*-mediated plant transformation. *Trends in Plant Science* **7**: 193–195.

Karpov PA, Rayevsky AV, Blume YB. 2010. Bioinformatic search for plant homologs of the protein kinase Bub1, a key component of the mitotic spindle assembly checkpoint. *Cytology and Genetics* **44**: 376–388.

Kerscher O, Crotti LB, Basrai MA. 2003. Recognizing chromosomes in trouble: association of the spindle checkpoint protein Bub3p with altered kinetochores and a unique defective centromere. *Molecular and Cellular Biology* **23**: 6406–6418.

Khodjakov A, Rieder CL. 2009. The nature of cell-cycle checkpoints: facts and fallacies. *Journal of Biology* **8**: 88.

Kimbara J, Endo TR, Nasuda S. 2004. Characterization of the genes encoding for MAD2 homologues in wheat. *Chromosome Research* **12**: 703–714.

Kitagawa R, Rose AM. 1999. Components of the spindle-assembly checkpoint are essential in *Caenorhabditis elegans*. *Nature Cell Biology* **1**: 514–521.

Kiyomitsu T, Murakami H, Yanagida M. 2011. Protein interaction domain mapping of human kinetochore protein Blinkin reveals a consensus motif for binding of spindle assembly checkpoint proteins Bub1 and BubR1. *Molecular and Cellular Biology* **31**: 998–1011.

Kiyomitsu T, Obuse C, Yanagida M. 2007. Human Blinkin/AF15q14 is required for chromosome alignment and the mitotic checkpoint through direct interaction with Bub1 and BubR1. *Developmental Cell* **13**: 663–676.

Kosetsu K, Matsunaga S, Nakagami H, Colcombet J, Sasabe M, Soyano T, Takahashi Y, Hirt H, Machida Y. 2010. The MAP kinase MPK4 is required for cytokinesis in *Arabidopsis thaliana*. *Plant Cell* **22**: 3778–3790.

Kurasawa Y, Earnshaw WC, Mochizuki Y, Dohmae N, Todokoro K. 2004. Essential roles of KIF4 and its binding partner PRC1 in organized central spindle midzone formation. *The EMBO Journal* **23**: 3237–3248.

Lampson MA, Kapoor TM. 2005. The human mitotic checkpoint protein BubR1 regulates chromosome-spindle attachments. *Nature Cell Biology* **7**: 93–98.

Lermontova I, Fuchs J, Schubert I. 2008. The Arabidopsis checkpoint protein Bub3.1 is essential for gametophyte development. *Frontiers in Bioscience* **13**: 5202–5211.

Lermontova I, Kuhlmann M, Friedel S, Rutten T, Heckmann S, Sandmann M, Demidov D, Schubert V, Schubert I. 2013. *Arabidopsis* KINETOCHORE NULL2 is an upstream component for centromeric histone H3 variant cenH3 deposition at centromeres. *Plant Cell* **25**: 3389–3404.

Lermontova I, Rutten T, Schubert I. 2011. Deposition, turnover, and release of CENH3 at Arabidopsis centromeres. *Chromosoma* **120**: 633–640.

Li R, Murray AW. 1991. Feedback control of mitosis in budding yeast. *Cell* **66**: 519–531.

Masoud K, Herzog E, Chabouté M-E, Schmit A-C. 2013. Microtubule nucleation and establishment of the mitotic spindle in vascular plant cells. *Plant Journal* **75**: 245–257.

Menges M, De Jager SM, Gruissem W, Murray JAH. 2005. Global analysis of the core cell cycle regulators of Arabidopsis identifies novel genes, reveals multiple and highly specific profiles of expression and provides a coherent model for plant cell cycle control. *Plant Journal* **41**: 546–566.

Meraldi P, Draviam VM, Sorger PK. 2004. Timing and checkpoints in the regulation of mitotic progression. *Developmental Cell* **7**: 45–60.

Müller S, Smertenko A, Wagner V, Heinrich M, Hussey PJ, Hauser M-T. 2004. The plant microtubule-associated protein AtMAP65-3/PLE is essential for cytokinetic phragmoplast function. *Current Biology* **14**: 412–417.

Musacchio A. 2011. Spindle assembly checkpoint: the third decade. *Philosophical Transactions of the Royal Society B* **366**: 3595–3604.

Musacchio A, Salmon ED. 2007. The spindle-assembly checkpoint in space and time. *Nature Reviews. Molecular Cell Biology* **8**: 379–393.

Pines J. 2011. Cubism and the cell cycle: the many faces of the APC/C. *Nature Reviews. Molecular Cell Biology* **12**: 427–438.

Rahmani Z, Gagou ME, Lefebvre C, Emre D, Karess RE. 2009. Separating the spindle, checkpoint, and timer functions of BubR1. *The Journal of Cell Biology* **187**: 597–605.

Sasabe M, Kosetsu K, Hidaka M, Murase A, Machida Y. 2011. *Arabidopsis thaliana* MAP65-1 and MAP65-2 function redundantly with MAP65-3/PLEIADE in cytokinesis downstream of MPK4. *Plant Signaling & Behavior* **6**: 743–747.

Sczaniecka M, Feoktistova A, May KM, Chen JS, Blyth J, Gould KL, Hardwick KG. 2008. The spindle checkpoint functions of Mad3 and Mad2 depend on a Mad3 KEN box-mediated interaction with Cdc20-anaphase-promoting complex (APC/C). *The Journal of Biological Chemistry* **283**: 23039–23047.

Smertenko AP, Kaloriti D, Chang H-Y, Fiserova J, Opatrny Z, Hussey PJ. 2008. The C-terminal variable region specifies the dynamic properties of *Arabidopsis* microtubule-associated protein MAP65 isotypes. *Plant Cell* **20**: 3346–3358.

Sudakin V, Chan GK, Yen TJ. 2001. Checkpoint inhibition of the APC/C in HeLa cells is mediated by a complex of BUBR1, BUB3, CDC20, and MAD2. *The Journal of Cell Biology* **154**: 925–936.

Suijkerbuijk SJE, van Dam TJP, Karagöz GE, von Castelmur E, Hubner NC, Duarte AMS, Vleugel M, Perrakis A, Rüdiger SGD, Snel B *et al.* 2012. The vertebrate mitotic checkpoint protein BUBR1 is an unusual pseudokinase. *Developmental Cell* **22**: 1321–1329.

Syrovatkina V, Fu C, Tran PT. 2013. Antagonistic spindle motors and MAPs regulate metaphase spindle length and chromosome segregation. *Current Biology* **23**: 2423–2429.

Talbert PB, Masuelli R, Tyagi AP, Comai L, Henikoff S. 2002. Centromeric localization and adaptive evolution of an *Arabidopsis* histone H3 variant. *Plant Cell* **14**: 1053–1066.

Taylor SS, Ha E, McKeon F. 1998. The human homologue of Bub3 is required for kinetochore localization of Bub1 and a Mad3/Bub1-related protein kinase. *The Journal of Cell Biology* **142**: 1–11.

Van Leene J, Hollunder J, Eeckhout D, Persiau G, Van De Slijke E, Stals H, Van Isterdael G, Verkest A, Neirynck S, Buffel Y *et al.* 2010. Targeted interactomics reveals a complex core cell cycle machinery in *Arabidopsis thaliana*. *Molecular Systems Biology* **6**: 397.

Vos JW, Pieuchot L, Evrard J-L, Janski N, Bergdoll M, de Ronde D, Perez LH, Sardon T, Vernos I, Schmit A-C. 2008. The plant TPX2 protein regulates prospindle assembly before nuclear envelope breakdown. *Plant Cell* **20**: 2783–2797.

Wang M, Tang D, Luo Q, Jin Y, Shen Y, Wang K, Cheng Z. 2012. BRK1, a Bub1-related kinase, is essential for generating proper tension between homologous kinetochores at metaphase I of rice meiosis. *Plant Cell* **24**: 4961–4973.

Wei Y, Multi S, Yang C-R, Ma J, Zhang Q-H, Wang Z-B, Li M, Wei L, Ge Z-J, Zhang C-H *et al.* 2011. Spindle assembly checkpoint regulates mitotic cell cycle progression during preimplantation embryo development. *PLoS ONE* **6**: e21557.

Yu HG, Muszynski MG, Kelly Dawe R. 1999. The maize homologue of the cell cycle checkpoint protein MAD2 reveals kinetochore substructure and contrasting mitotic and meiotic localization patterns. *The Journal of Cell Biology* **145**: 425–435.

Supporting Information

Additional supporting information may be found in the online version of this article.

Fig. S1 Comparison of BUBR1/MAD3 and BUB1-related proteins in plants, yeasts and vertebrates.

Fig. S2 Comparison of plant BUB1-related kinases and human BUB1.

Fig. S3 Interaction of MAP65-3 and SAC components *in planta*.

Fig. S4 RT-qPCR analysis of the expression of genes encoding SAC components during root-knot nematode infection.

Fig. S5 Similar morphologies of the wild-type, single, double and triple *mad3.1 mad3.2 brk1* mutants under normal growth conditions.

Fig. S6 Root-knot nematode infection is not altered in *mad3.1 mad3.2* and *brk1* mutants.

Fig. S7 Mitotic defects in *mad3.1 mad3.2* mutants.

Table S1 Primers used in this study

Please note: Wiley Blackwell are not responsible for the content or functionality of any supporting information supplied by the authors. Any queries (other than missing material) should be directed to the *New Phytologist* Central Office.